Electronic Supplementary Material (ESI) for CrystEngComm.

Electronic Regulation of $NiSe_2$ by Co doping for Accelerating Hydrogen Evolution Reaction

Huakai Xu, Kebin Lu, Chuanhai Jiang, Xiaofei Wei, Zhifei Wang, Yuguo Ouyang, Fangna Dai*

School of Materials Science and Engineering, China University of Petroleum (East China), Qingdao 266580, China

*Corresponding Author: fndai@upc.edu.cn.

Theoretical calculation

The theoretical calculations in the DFT framework was based on the VASP package. Exchange correlation energies were treated using a generalized gradient approximation with the Perdew–Burke–Ernzerhof function (GGA-PBE). Projector-augmented wave potential was used to describe the ion-electron interaction, and the plane wave cutoff energy was set to 350 eV. The k-point sampling was obtained from the Monkhorst−Pack scheme with a (3 × 3 × 1) mesh for optimization and a (20 × 20 × 1) mesh for DOS calculation. The geometry optimization and energy calculation are finished when the electronic self-consistent iteration and force were reach 10^{-4} eV and 0.01 eV·Å^{-1}, respectively.

The structure was modelled from the NiSe2 (0 0 1) and CoSe2 (0 0 1) plane, the supercell with a lattice constant of 14.3 Å × 14.5 Å is consisted of 96 atoms separated by a vacuum region of 15 Å along the direction normal to the sheet plane to avoid strong interactions. In the process of structural optimization, the bottom atom of catalyst is fixed and only the upper two layers are released.

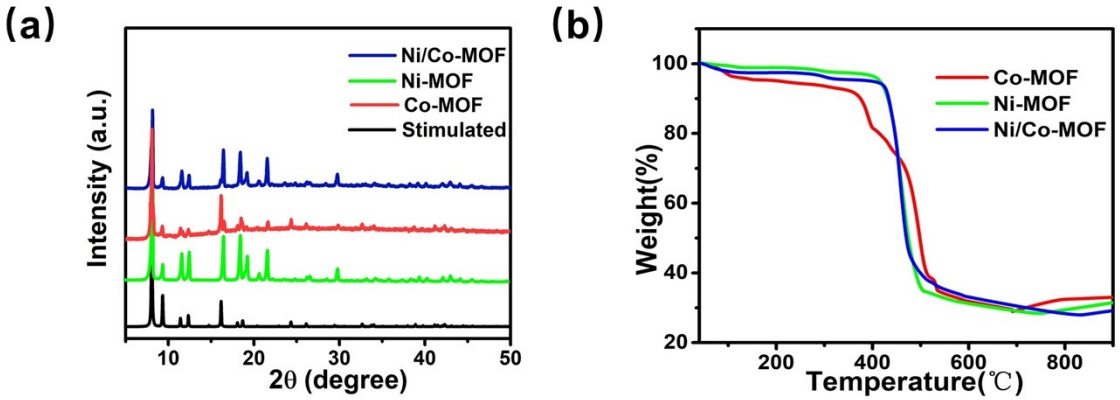

Figure S1 (a) XRD patterns; (b) TGA of MOF nanosheets.

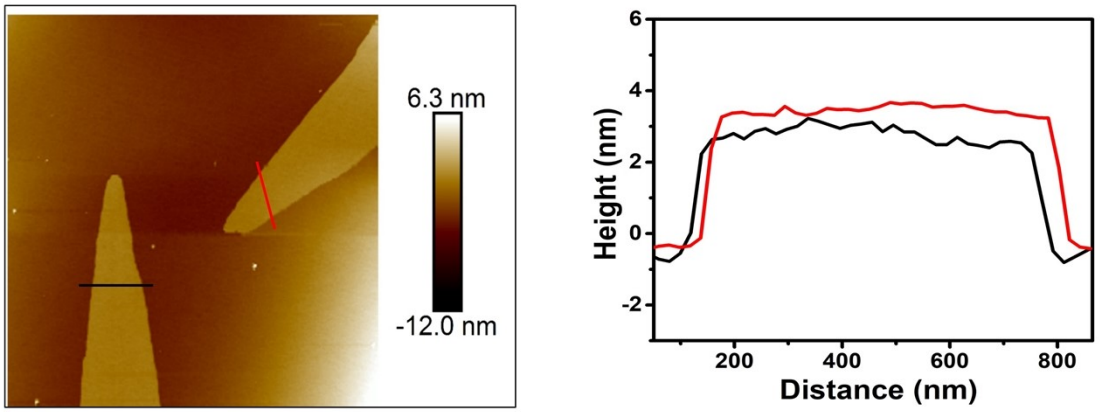

Figure S2. AFM images of ultrathin MOF nanosheets

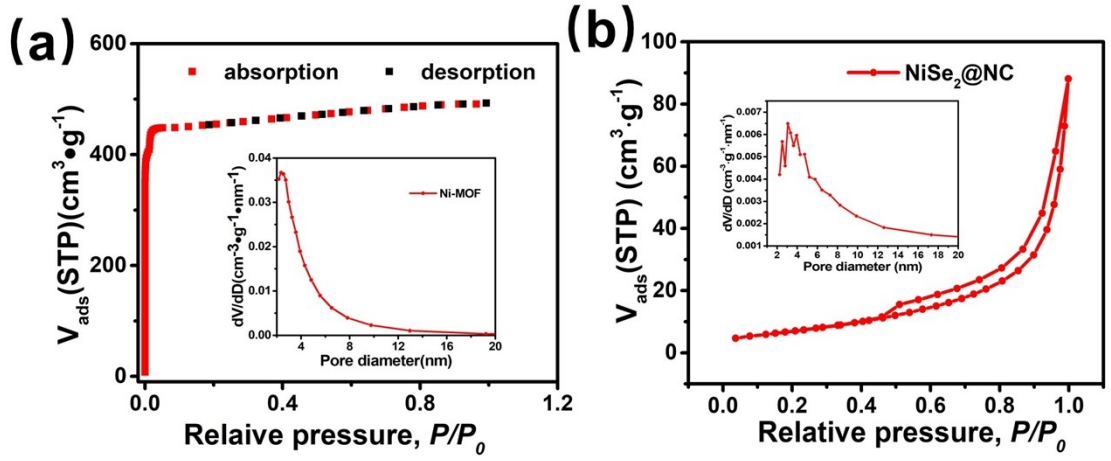

Figure S3. (a) N_2 adsorption-desorption isotherms of ultrathin layered Ni-MOF and $NiSe_2$@NC (The illustration shows the pore size distribution diagram).

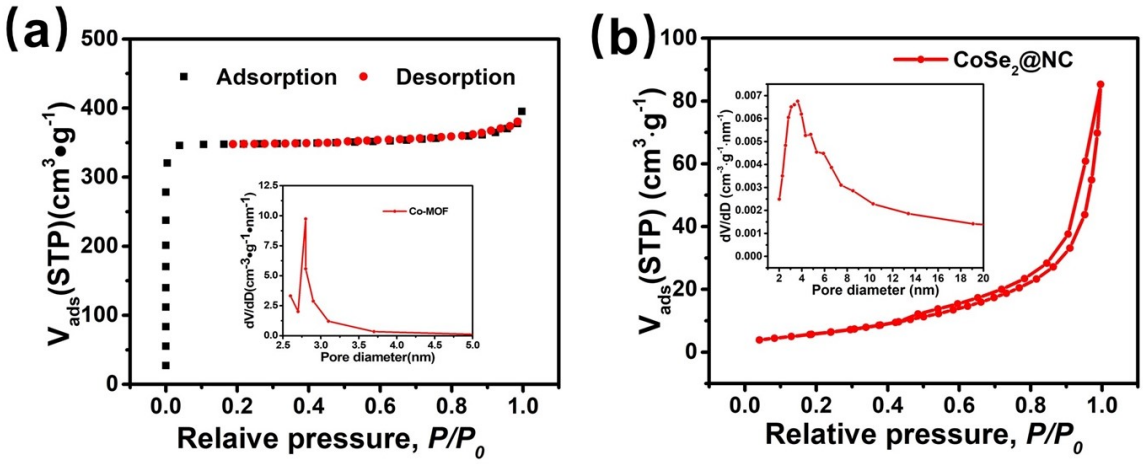

Figure S4. (a) N_2 adsorption-desorption isotherms of ultrathin layered Co-MOF and $CoSe_2$@NC (The illustration shows the pore size distribution diagram).

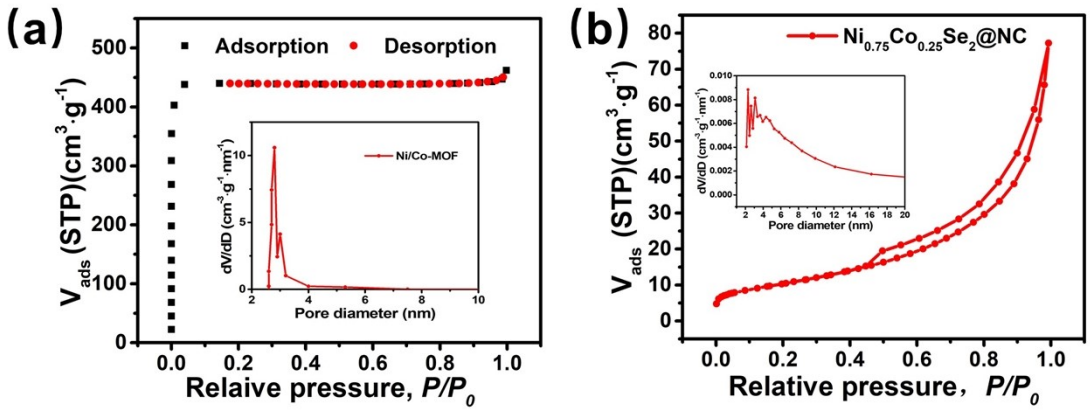

Figure S5. (a) N_2 adsorption-desorption isotherms of ultrathin layered Ni/Co-MOF and $Ni_{0.75}Co_{0.25}Se_2$@NC (The illustration shows the pore size distribution diagram).

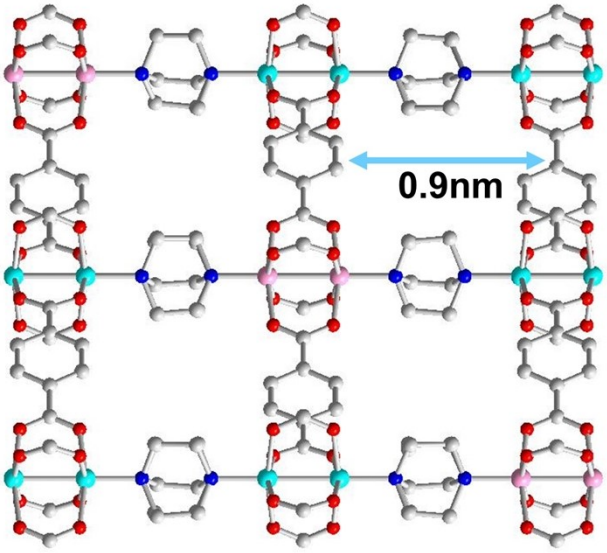

Figure S6. The pillar-layered structure of ultrathin layered MOF (Ni, blue; Co, pink N, deep blue; O, red; C, gray).

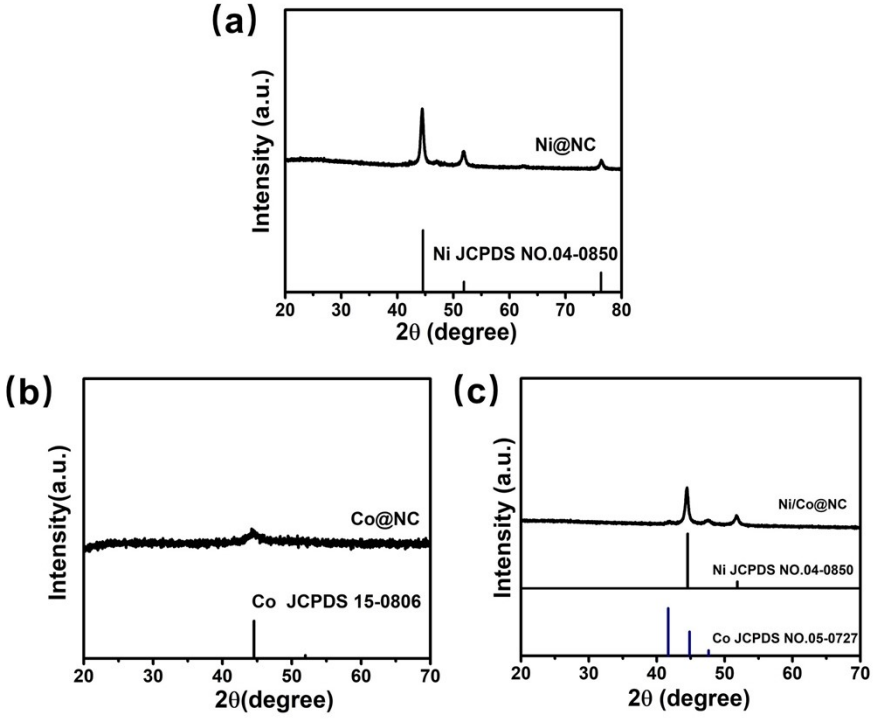

Figure S7 XRD pattern of Ni@NC, Co@NC, Ni/Co@NC

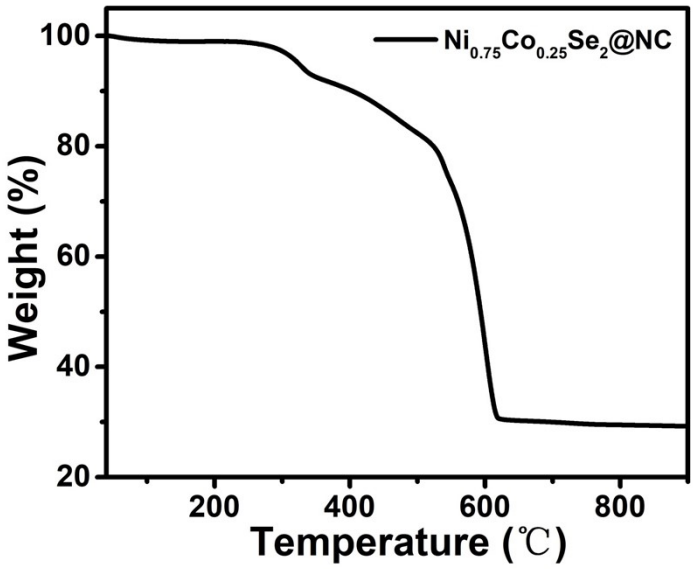

Figure S8 TGA curve of $Ni_{0.75}Co_{0.25}Se_2$@NC nanomaterials performed in the O_2 atmosphere.

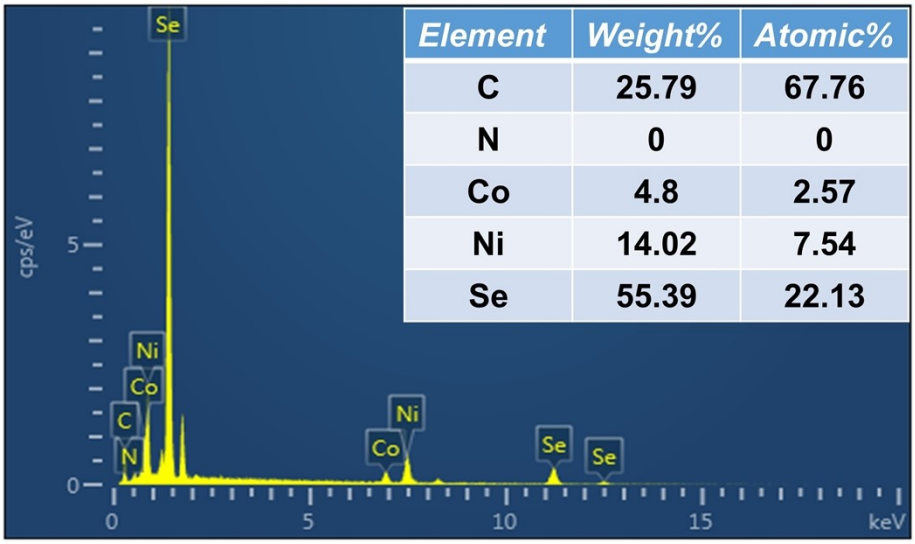

Element	Weight%	Atomic%
C	25.79	67.76
N	0	0
Co	4.8	2.57
Ni	14.02	7.54
Se	55.39	22.13

Figure S9. Energy dispersive spectra of $Ni_{0.75}Co_{0.25}Se_2$@NC nanomaterials.

Elements	Molar ratio（Ni：Co)
Ni Co	1.004：0.33027

Figure S10 Elements percentage of $Ni_{0.75}Co_{0.25}Se_2$@NC obtained from ICP-OES

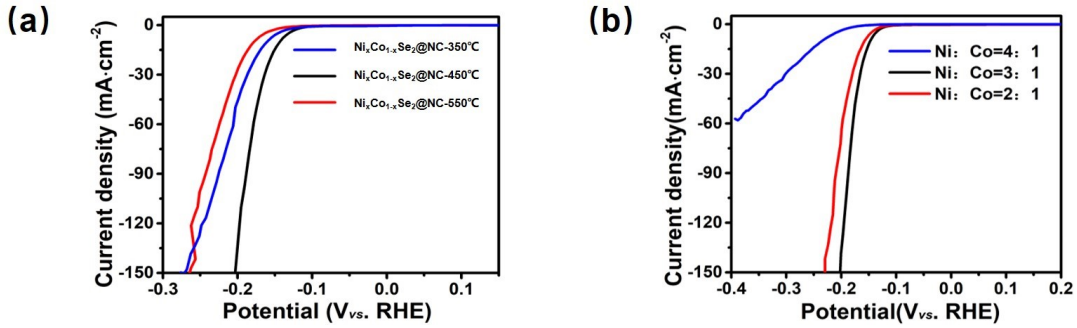

Figure S11 LSV curves for $Ni_{0.75}Co_{0.25}Se_2$@NC: (a) with different mass ratios of Ni and Co (2:1, 3:1, 4:1); (b) with different synthesis temperature (350℃, 450℃ and 550℃)

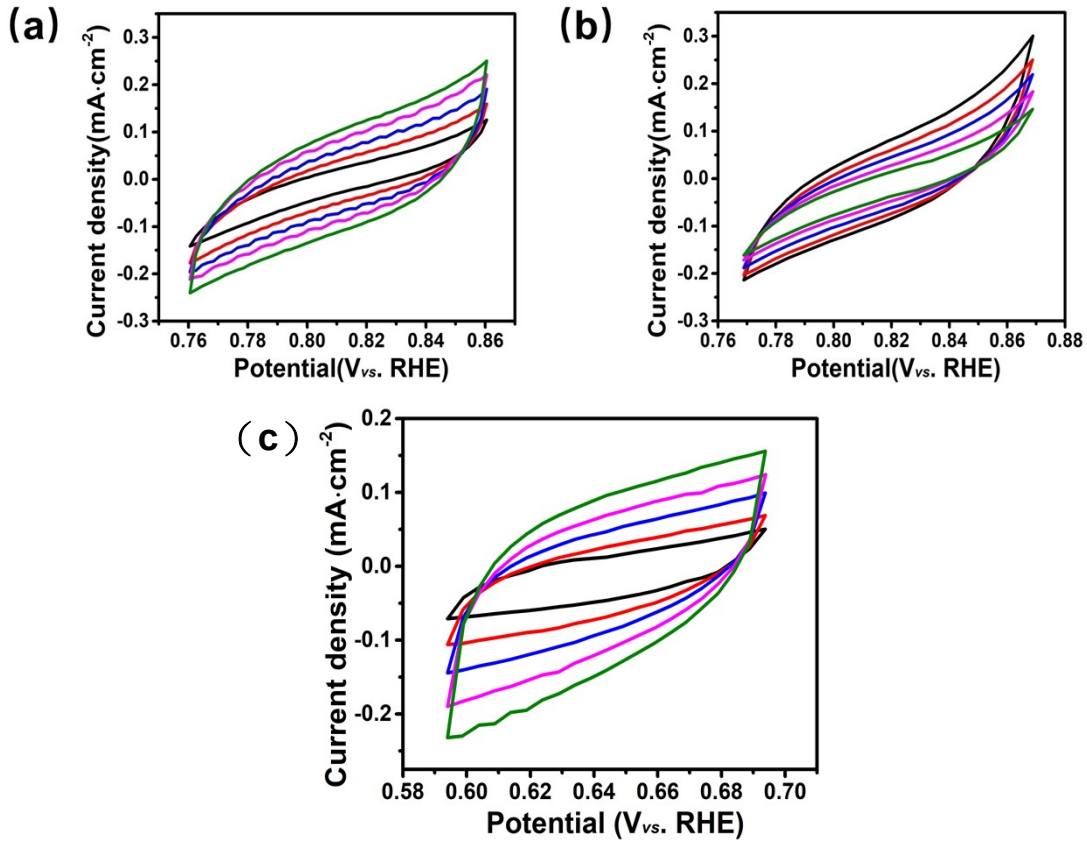

Figure S12. The CV curves of (a) $CoSe_2$@NC, (b) $NiSe_2$@NC and (c) $Ni_{0.75}Co_{0.25}Se_2$@NC.

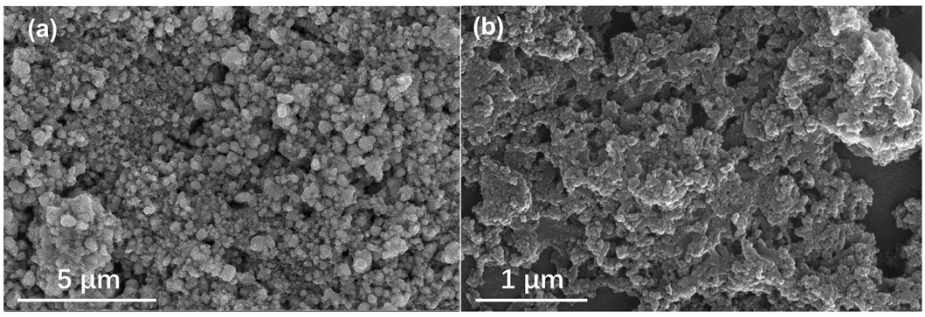

Figure S13 The SEM of $Ni_{0.75}Co_{0.25}Se_2$@NC (a) before and (b) after stability test.

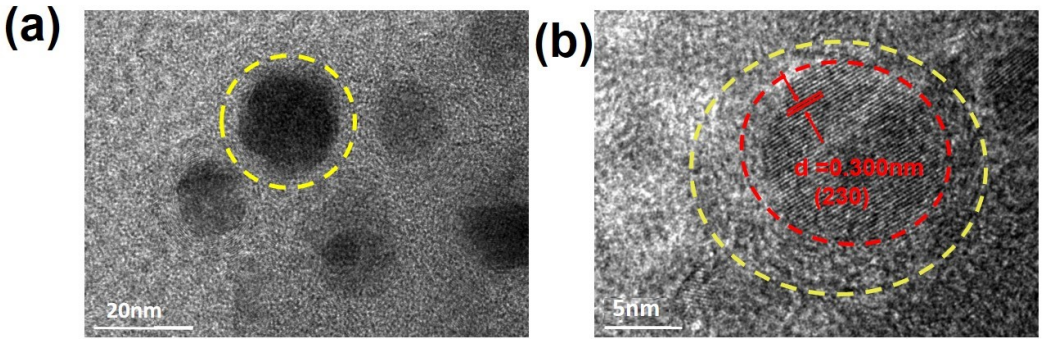

Figure S14 the TEM and HR-TEM of $Ni_{0.75}Co_{0.25}Se_2$@NC after stability test.

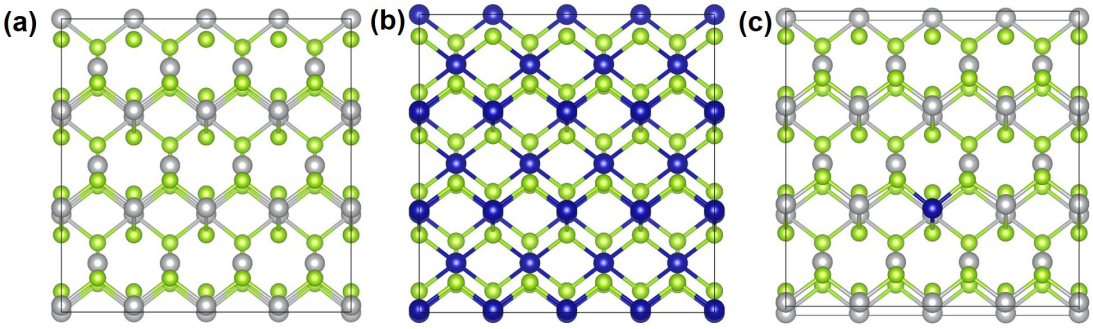

Figure S15 the model of (a) $NiSe_2$, (b) $CoSe_2$, (c) Co1-$NiSe_2$.

Table S1. Comparison of HER catalytic activity of different Co-doped catalysts in 0.5 M H_2SO_4

HER catalysts	E10 (mV)	Tafel slope ($mV \cdot dec^{-1}$)	Electrolyte	Ref.
$Ni_{0.75}Co_{0.25}Se$@NC	143	37.5	0.5 M H_2SO_4	This work
Co-MoS_2/rGO	147	49.5	0.5 M H_2SO_4	[1]
$Fe_{0.7}Co_{0.3}Se$/RGO-12	166	36	0.5 M H_2SO_4	[2]
Co10%-VS_2	234	93	0.5 M H_2SO_4	[3]
Co13%-NiS_2/CoS_2	162.3		0.5 M H_2SO_4	[4]
Co-$MoSe_2$	217	65	0.5 M H_2SO_4	[5]
Co-$^{S}MoS_2$	220	92	0.5 M H_2SO_4	[6]
$Co_xMo_{1-x}S_2$	357	120	0.5 M H_2SO_4	[7]
Co-VSe_2	230	36.1	0.5 M H_2SO_4	[8]
Co-WSe_2/MWNTs	147	37	0.5 M H_2SO_4	[9]
$Ni_{1/3}Co_{2/3}Se_2$	145	46.3	0.5 M H_2SO_4	[10]

REFERENCES

[1] J. W. Ma, A. Cai, X. L. Guan, K. Li, W. C. Peng, X. B. Fan, G. L. Zhang, F. B. Zhang and Y. Li, *Int. J. Hydrog. Energy*, 2020, **45**, 9583-9591.

[2] X. W. Xu, Y. C. Ge, M. Wang, Z. Q. Zhang, P. Dong, R. Baines, M. X. Ye and J. F. Shen, *ACS Appl. Mater. Interfaces*, 2016, **8**, 18036-18042.

[3] M. X. Zhao, M. Y. Yang, W. J. Huang, W. C. Liao, H. D. Bian, D. Z. Chen, L. Wang, J. N. Tang and C. Liu, *ChemCatChem*, 2021, **13**, 2138-2144.

[4] Z. H. Peng, S. Lou, Y. Gao, L. J. Kong, S. C. Yan, K. Wang and H. Z. Song, *Nanomaterials*, 2021, **11**, 1245.

[5] O. Zimron, T. Zilberman, S. R. Kadam, S. Ghosh, S. –L. Kolatker, A. Neyman, R. Bar-Ziv and M. Bar-Sadan, *Isr. J. Chem.* 2020, **60**, 624-629.

[6] T. Lau, X. W. Lu, J. Kulhavy, S. Wu, L. L. Lu, T. –S. Wu, R. Kato, J. Foord, Y.-L. Soo, K. Suenag and S. C. E. Tsang, *Chem. Sci.*, 2018, **9**, 4769-4776.

[7] J. Pan, C. S. Song, X. Wang, X. T. Yuan, Y. Q. Fang, C. G. Guo, W. Zhao and F. Q. Huang, *Inorg. Chem. Front.*, 2017, **4**, 1895.

[8] Q. Zhu, M.M. Shao, S. H. Yu, X. N. Wang, Z. Tang, B. Chen, H. Cheng, Z. G. Lu, D. Chua H. Pan, *ACS Appl. Energy Mater.*, 2019, **2**, 644-653.

[9] X. L. Zheng, G. Y. Zhang, X. P. Xu, L. Liu, J. N. Zhang and Q. Xu, *Appl. Surf. Sci.*, 2019, **496**, 143694.

[10] Z. Zhang, Y. D. Liu, L. Ren, H. Zhang, Z. Y. Huang, X. Qi, X. L. Wei and J. X. Zhong, *Electrochim. Acta*, 2016, **200**, 142-151.